International Journal of Psychophysiology 218 (2025) 113283

Contents lists available at ScienceDirect

International Journal of Psychophysiology

journal homepage: www.elsevier.com/locate/ijpsycho

Theta-frequency transcranial alternating current stimulation enhances proactive control in individuals

Lei Wang [a], YuHong Ou [a], Renlai Zhou [a,b,c,*]

[a] Department of Psychology, Nanjing University, Nanjing, 210023, China
[b] Department of Radiology, Nanjing Drum Tower Hospital, the Affiliated Hospital of Nanjing University Medical School, Nanjing, 210008, China.
[c] State Key Laboratory of Media Convergence Production Technology and Systems, Beijing, 100083, China

ARTICLE INFO

Keywords:
Proactive control
DLPFC
Theta
Neuroplasticity
Fluid intelligence

ABSTRACT

Proactive control is defined as the capacity of an individual to selectively allocate attentional resources to task-relevant cues during the preparatory phase of a task, actively encode and sustain this information within working memory, and subsequently establish appropriate response readiness. Research demonstrates that proactive control has neuroplasticity. The dorsolateral prefrontal cortex (DLPFC) is critically implicated in the modulation of proactive control. Theta oscillations, functioning as a neural gating mechanism, facilitate the preferential allocation of attentional resources toward the processing of memory-relevant information, thereby enhancing the maintenance of such information and playing a pivotal role in memory encoding and cognitive resource distribution. The present study employed theta-frequency transcranial alternating current stimulation (tACS) targeting the DLPFC to further elucidate the neuroplasticity of proactive control. Concurrently, to investigate the relationship between fluid intelligence and proactive control, participants' fluid intelligence was assessed pre- and post-stimulation. A cohort of 58 participants was randomly assigned to receive either left DLPFC stimulation ($n = 29$) or right DLPFC stimulation (n = 29). The results revealed that stimulation of the left DLPFC significantly enhanced participants' proactive control capabilities. In ERP indicators, the CNV, following active stimulation, the CNV in the BX condition was significantly greater than that in the pre and sham stimulation ($p \leq 0.006$). In behavioral outcomes, the accuracy rate for the BX condition was significantly higher after active stimulation compared to that in pre-stimulation and sham stimulation ($p \leq 0.017$). In the lDLPFC group, fluid intelligence performance was significantly enhanced, and fluid intelligence scores after active stimulation were significantly higher compared to those during pre and sham stimulation ($p \leq 0.032$). A statistically significant correlation was observed between participants' proactive control capabilities and fluid intelligence. In the rDLPFC group, no significant changes in any of the indicators were observed. These findings underscore the efficacy of neuromodulatory interventions targeting the left DLPFC in augmenting proactive control and suggest a dynamic interplay between proactive control and fluid intelligence.

1. Introduction

Cognitive control facilitates goal-directed behavior by enabling individuals to regulate their cognitive, behavioral, emotional, and motivational processes (Cocchi et al., 2013; Diamond, 2013; Zink et al., 2021). In recent years, some researchers have argued that traditional inhibitory control theory primarily emphasizes an individual's ability to suppress behaviors when facing interference or dominant responses, while failing to adequately highlight the proactive aspect of the inhibition process itself (Braver et al., 2007). Braver's Dual Mechanisms of Cognitive Control (DMC) theory proposes that cognitive control operates through two distinct modes: proactive control and reactive control. Proactive control is conceptualized as a form of "early selection," involving the selective attentional processing of task-relevant cues during the pre-task phase and the active maintenance of these cues to prepare for appropriate responses. For instance, prior to engaging in a task, individuals gather and analyze pertinent information to formulate an action plan. Proactive control is cue-driven and heavily influenced by top-down information processing (Braver et al., 2007). In contrast, reactive control refers to the flexible utilization of task-relevant information that emerges at the moment of response to resolve conflicts. When prior cues are required to address current conflicts, reactive

* Corresponding author at: Department of Psychology, Nanjing University, Room 418, Heren Hall, 163 Xianlin Avenue, Nanjing, 210023, China.
E-mail address: rlzhou@nju.edu.cn (R. Zhou).

https://doi.org/10.1016/j.ijpsycho.2025.113283
Received 6 July 2025; Received in revised form 24 October 2025; Accepted 27 October 2025
Available online 30 October 2025

control involves retrieving and reactivating these cues to guide responses and correct potential error tendencies. For example, during task execution, new information may arise, and reactive control allows for the adaptive integration of this information to facilitate ongoing activities. When such information conflicts with prior knowledge, reactive control enables the retrieval of earlier information to resolve the conflict. Reactive control is probe-driven and predominantly influenced by bottom-up information input (Braver et al., 2007). This DMC provides a comprehensive understanding of the mechanisms underlying cognitive control and its adaptive functions in goal-directed behavior.

In cognitive tasks, individuals are required to dynamically balance proactive and reactive control mechanisms based on task demands, environmental context, and individual capabilities, thereby optimizing their cognitive control strategies for task performance. Proactive control, distinguished by its anticipatory, top-down nature and efficient processing of task-related rules, has been empirically established as a more effective cognitive control strategy (Braver et al., 2007, 2009). As a result, a substantial body of research has focused on developing and implementing interventions aimed at enhancing individuals' proactive control capacities. For example, Edwards et al. (2010) demonstrated that individuals diagnosed with schizophrenia could significantly improve their utilization of proactive control strategies through targeted training, achieving cognitive control patterns comparable to those observed in healthy adults. Similarly, interventions designed to train older adults in the deliberate application of predictive cues during task execution have been shown to markedly enhance their proactive control abilities (Braver et al., 2009; Paxton et al., 2006). Furthermore, the efficacy of techniques such as mindfulness training and transcranial direct current stimulation (tDCS) has been consistently corroborated across multiple studies, underscoring the high degree of plasticity inherent in individuals' proactive control capacities (Boudewyn et al., 2020; Li et al., 2018).

The dorsolateral prefrontal cortex (DLPFC) constitutes a pivotal component of the cognitive control network, playing a critical role in the active maintenance of goal-directed and task-set information. Studies have shown that the DLPFC exhibits sustained pre-stimulus activation across a diverse array of tasks, particularly in contexts involving cross-trial interference induced by frequent stimulus switching. This activation pattern is hypothesized to reflect the neural mechanisms underlying the active maintenance of task rules (MacDonald 3rd et al., 2000; Miller and Cohen, 2001; Sakai and Passingham, 2006). Furthermore, research has identified a functional asymmetry between the left DLPFC (lDLPFC) and the right DLPFC (rDLPFC), with the lDLPFC appearing to play a more prominent role in proactive control. For example, a study employing tDCS on the lDLPFC in individuals with schizophrenia revealed that 20 min of anodal tDCS significantly enhanced task performance, with participants demonstrating improved proactive control through effective cue maintenance strategies (Boudewyn et al., 2020). Conversely, another tDCS study found that anodal stimulation of the rDLPFC did not yield comparable improvements in proactive control, while cathodal stimulation impaired the active maintenance of task-related cues (Gomez-Ariza et al., 2017). These findings underscore the differential functional contributions of the lDLPFC and rDLPFC to cognitive control processes.

The execution of cognitive tasks in the brain necessitates the involvement of extensive neuronal assemblies, with neural oscillations reflecting the sustained and rhythmic activity of these assemblies, thereby facilitating efficient information exchange among different neuronal clusters. Research indicates that the coordinated integration of multiple brain regions is achieved through neural oscillations (Zhang et al., 2018). Prior studies have revealed that the top-down cognitive control process is usually associated with the phenomenon of theta-frequency oscillation synchronization. For instance, the maintenance and manipulation of information in working memory are often accompanied by synchronous theta activity (Klimesch et al., 2006; Jacobs et al., 2006), and the successful encoding and recollection of items are related to the current theta phase (Rizzuto et al., 2006). Reasonable allocation of cognitive resources according to needs is also associated with a greater degree of inter-regional theta synchronization or consistency (Mizuhara and Yamaguchi, 2007). Successful inhibitory control in cognitive tasks is associated with increased midfrontal theta oscillations. These midfrontal theta oscillations are thought to reflect the neural mechanisms underlying conflict detection (Cavanagh and Frank, 2014; Eisma et al., 2021). Additionally, theta oscillations have been implicated in various cognitive control tasks and are considered potential neural markers of cognitive effort and the implementation of top-down control. Interregional synchronization of theta oscillations in the frontoparietal network(FPN) is associated with cognitive control. Accumulating evidence demonstrates that this synchronization enhances behavioral performance in control tasks, particularly during rule-set switching (Goense and Logothetis, 2008; Koch et al., 2009). A repetitive transcranial magnetic stimulation (rTMS) study demonstrated that theta-frequency rTMS applied to the lDLPFC during the maintenance phase of a working memory task significantly enhanced the brain's prioritization of memorized information, thereby improving working memory capacity for target information in the right visual field. This finding suggests that frontal theta oscillations regulate the allocation of cognitive resources toward the prioritized processing of memory-related information (Force et al., 2021). The above evidence indicates that theta wave oscillations play a unique role in controlling the combination of neural units, facilitating information integration and enabling goal-directed control processes (Sauseng et al., 2010). Consequently, investigating whether enhancing theta-frequency activity in the DLPFC can strengthen an individual's proactive control capacity is a central focus of this study.

Recent research has demonstrated that the modulation of neural oscillations in the brain can be accomplished through the phenomenon of “neural entrainment.” This process entails the interaction between rhythmic external stimuli and the corresponding rhythmic neural oscillations within specific brain regions, culminating in synchronization and the subsequent regulation of internal neural oscillatory activity (Wischnewski et al., 2022). Techniques such as repetitive rTMS and transcranial alternating current stimulation (tACS) are particularly effective in inducing specific frequency bands of neural oscillations in targeted brain areas with high precision. As a result, these methodologies are extensively utilized in research to elucidate the specific roles of neural oscillations in cognitive tasks (Antal et al., 2008). In the present study, high-precision tACS will be employed to administer theta-frequency stimulation to the dorsolateral prefrontal cortex (DLPFC) of participants, with the objective of augmenting their proactive control capabilities.

The cue-probe AX continuous performance task (AX-CPT) effectively differentiates between proactive and reactive control in individuals (Cohen et al., 1999). This paradigm comprises cue stimuli (A or B) and probe stimuli (X or Y), with a blank screen presented as an interstimulus interval (ISI) separating these probes, forming four distinct sequence pairs. Participants are instructed to respond solely to the high-frequency sequence (e.g., the AX pairs, which occurs with a 58 % probability), while refraining from responding to the three low-frequency sequences (AY, BX, and BY, each with a 14 % probability). Consequently, the high-frequency sequence serves as an effective cue (A), prompting participants to respond swiftly and accurately to the subsequent stimulus (X), thereby establishing a response bias. In the context of the BX sequence, individuals employ proactive control strategies, actively maintaining the cue to mitigate the false alarm rate associated with the BX pairs. Conversely, during the AY sequence, the elevated frequency of cue A heightens participants' response bias toward the subsequent probe stimulus, necessitating enhanced conflict monitoring when probe stimulus Y is presented. This increased response bias escalates the cost of response inhibition. Thus, the reaction times and accuracy rates for the BX and AY sequences serve as indicators of participants' proactive and reactive control capabilities. Furthermore, the *d*’ Context indices

provide a measure of participants' sensitivity to task cues. A higher *d'* signifies more robust proactive control abilities (Braver, 2012).

Behavioral measures are insufficient to fully capture the changes in participants following an intervention. In cognitive neuroscience research, the utilization of proactive control strategies is closely associated with sustained neural activation during the cue-stimulus interval. The ERP component Contingent Negative Variation (CNV), first identified by Walter et al. (1964) during reaction time studies, serves as an electrophysiological marker indexing proactive preparation for upcoming tasks in both motor and attentional domains. Higher CNV amplitudes are indicative of more extensive and active preparation (Karayanidis and Jamadar, 2014; Shen et al., 2018; Smith et al., 2006). Research has revealed that CNV is a negative amplitude associated with motor preparation that emerges in response to the "cue stimulus", and this brain activity is believed to be influenced by motivation and effort levels (Zhang et al., 2017). This component reflects the degree of conscious or unconscious proactive preparation in cognitive activities. Studies have shown that the use of proactive control strategies is associated with sustained brain activation during the interval between cue-probe presentation. In the AX-CPT task, the CNV in the medial frontal regions during the cue-locked is related to anticipatory attention (Brunia, 1999) or response preparation processes (Karayanidis and Jamadar, 2014). Researchers hypothesize that the amplitude of the CNV may reflect neuronal activation during the accumulation of temporal scales, with increased allocation of attentional resources leading to greater neuronal activation intensity and higher amplitude (Macar et al., 1999). When individuals exhibit a higher amplitude CNV in response to a specific cue, it indicates that they are engaging in more proactive preparation for subsequent reactions (Shen et al., 2018; Smith et al., 2006). Upon the presentation of a probe stimulus, individuals engage in cognitive monitoring, which is reflected in the emergence of a negative deflection component known as N2. The amplitude of the N2 component is a reliable index of inhibitory control and conflict monitoring capabilities (Hämmerer et al., 2010; Lo, 2018; Nieuwenhuis et al., 2003; Van Veen and Carter, 2002; Pires et al., 2014). This component underscores the top-down regulation of conflict and the allocation of cognitive resources to inhibitory control tasks (Nieuwenhuis et al., 2003; Pires et al., 2014). Moreover, the amplitude of the N2 component is modulated by the efficiency of inhibitory control, with greater efficiency associated with reduced amplitudes (Lo, 2018). Subsequent to stimulus onset, the P3 component, which reflects inhibitory costs, typically emerges within a latency window of 300–500 ms (Bruin and Wijers, 2002; Pfefferbaum et al., 1985). The P3 component is hypothesized to signify a transition from reactive to proactive control strategies (Casey et al., 2000; Church et al., 2017).

There is a significant positive correlation between an individual's proactive control capacity and fluid intelligence. Fluid intelligence refers to reasoning and novel problem-solving abilities. Studies have demonstrated that individuals with higher fluid intelligence exhibit enhanced proactive control capabilities, enabling them to more effectively implement proactive control strategies when confronted with cognitive tasks (Burgess et al., 2011). This relationship has been corroborated in developmental research involving children. In a study by Rico-Picó et al. (2021), children with high fluid intelligence exhibited significantly greater CNV than those with low fluid intelligence; and these children demonstrated better behavioral indices of proactive control, together with increased brain preparation to response cues. Nevertheless, the extant literature does not provide evidence regarding the dynamic interplay between proactive control capacity and fluid intelligence. Consequently, fluid intelligence scores will be operationalized as a measure of intervention transfer effects to further investigate the nature of this relationship.

In summary, we hypothesize that theta-frequency tACS applied to the lDLPFC can enhance proactive control capacity. To evaluate the efficacy of this intervention, the present study employs a comparative design, examining behavioral performance and ERPs during the AX-CPT task across three conditions: lDLPFC pre-stimulation, sham stimulation, active stimulation; and rDLPFC pre-stimulation, sham stimulation, active stimulation. Specifically, successful intervention is expected to yield improved accuracy rates in both AX and BX trial types, as well as an enhanced *d'* Context indices. At the neurophysiological level, effective stimulation is hypothesized to result in a significant increase in CNV amplitude during BX pairs, a marked reduction in N2 amplitude in both AX and BX trials, and the potential elicitation of larger P3 components in AY and BX trials. Furthermore, a significant improvement in fluid intelligence scores is anticipated following the successful enhancement of proactive control capacity.

2. Method

2.1. Participants

Participants were recruited via online platforms, with eligibility restricted to university students. The screening protocol incorporated the Beck Anxiety Inventory (BAI), and the Beck Depression Inventory (BDI) to ensure participants did not exhibit clinically significant levels of anxiety or depression. 66 individuals completed the screening questionnaires, from which 60 were selected for participation in the experimental protocol. Due to data quality concerns, responses from 2 participants were excluded from the final analysis. The resultant sample comprised 58 participants, with 29 individuals assigned to the left dorsolateral prefrontal cortex (lDLPFC) stimulation condition (mean age = 18.73 ± 1.2 years, 14 females) and 29 individuals assigned to the right dorsolateral prefrontal cortex (rDLPFC) stimulation condition (mean age = 18.75 ± 1.05 years, 17 females). All participants recruited for the study were right-handed, and individuals with a history of psychiatric disorders, psychotropic medication use, brain injury, or craniotomy were systematically excluded. Prior to participation, all individuals provided written informed consent after being fully briefed on the experimental procedures, potential implications, and their right to withdraw at any point without penalty. Participants were compensated appropriately upon completion of the study. The research protocol received ethical approval from the Ethics Committee of the Department of Psychology at Nanjing University.

2.2. Procedure

Participants underwent three testing sessions—pre-test, sham tACS, and active tACS—administered in a counterbalanced order to mitigate potential order effects, and participants were effectively blinded to the stimulation conditions. A 28-day interval was maintained between sessions to ensure that female participants were tested on the same phase of their menstrual cycle (To maintain consistency, male participants also had a 28-day interval between sessions). This design consideration is supported by evidence indicating that fluctuations in sex hormones across menstrual phases modulate cognitive responses in females (Amin et al., 2006). Specifically, elevated levels of estrogen and progesterone are associated with enhanced mood states and increased prefrontal cortical activation. During the tACS sessions, participants received 20 min of stimulation, with the sham condition limited to 30 s of stimulation. In the pre-test and after each stimulations, participants completed an AX-CPT task with ERP recordings and the Raven's Advanced Progressive Matrices (RAPM) to evaluate changes in proactive control capacity and fluid intelligence. At the conclusion of the experimental protocol, participants completed a self-report questionnaire assessing physiological sensations during stimulation to ensure the absence of adverse effects.

2.3. HD-tACS

HD-tACS was administered via a 4 + 1 multi-channel configuration, powered by a dedicated battery unit (Model 9002 A, Soterix Medical

Inc.). During the active stimulation protocol, a bipolar sinusoidal current at a frequency of 6 Hz was delivered to the lDLPFC or the rDLPFC. The current intensity was incrementally increased to 2 mA over a 30-s ramp-up period at the onset of stimulation and sustained until the end of the 20-min stimulation period, followed by a 30-s ramp-down period to 0 mA (Tavakoli and Yun, 2017; Zhu et al., 2023). In the sham stimulation, the current was similarly increased to 2 mA over 30 s, then gradually reduced to 0 mA over the subsequent 30 s, and remained at 0 mA for the duration of the session. Electrode placement was standardized according to the international 10–20 system, with the central electrodes positioned at F3 (lDLPFC) and F4 (rDLPFC), and the four return electrodes located at F5, F1, FC3, and AF3 for lDLPFC, and F6, F2, FC4, and AF4 for rDLPFC (Thair et al., 2017; Tavakoli and Yun, 2017; Zhu et al., 2023). To ensure optimal conductivity, impedance at each electrode was maintained below 5 kΩ throughout the stimulation period. This was achieved using five Ag/AgCl electrodes (outer diameter: 12 mm, inner diameter: 6 mm) housed in plastic electrode holders filled with conductive gel. The current flow was simulated and showed a specific effect of the stimulation on the dlPFC, as shown in Figs. 1A and B. Upon completion of the experimental protocol, all participants were required to complete a questionnaire to evaluate their subjective experience of the stimulation. (see Fig. 1A and 1B).

2.4. Task

2.4.1. RAPM

The RAPM represents an advanced iteration of the Raven's Progressive Matrices (Raven, 1990), specifically designed to evaluate fluid intelligence in individuals aged 16 and above who possess a high school education. The RSPM is extensively employed in diverse assessments of fluid intelligence (Sternberg et al., 1996). The correlation coefficient between RAPM and the Wechsler Adult Intelligence Scale-Revised (WAIS-R) is $r = 0.56$ ($p < 0.05$, $N = 97$) (Jaušovec and Jaušovec, 2012), and it also exhibits a correlation ranging from 0.40 to 0.75 with RSPM (Court and Raven, 1995). Consequently, the utilization of RAPM does not significantly modify its effectiveness in measuring fluid intelligence. Participants completed the test via a paper-based workbook.

2.4.2. AX-CPT

The experimental task in this study utilized the AX-CPT paradigm, structured into four blocks, each containing 100 trials. Each trial was composed of a cue and a probe. In this task, cue A was represented by a blue square; probe X by a yellow square; cue B by either a green or red square; and probe Y by either a green or purple square. These color blocks formed four distinct pairs: AX (blue-yellow), AY (blue-purple), BX (green-yellow), and BY (red-green). The AX pairs constituted 58 % of all trials (232 trials), while each of the AY, BX, and BY pairs accounted for 14 % of the trials (56 trials each). Participants were instructed to press the F key upon the presentation of the AX pairs and the J key for the other three pairs. The detailed procedure is depicted in Fig. 2. The experiment commenced with a fixation point "+"(3 mm × 3 mm) displayed at the center of the screen for a duration of 1000-1500 ms, followed by a 300 ms cue stimulus (80 mm × 80 mm), and subsequently a 600 ms blank screen. Following the blank screen, another fixation point (3 mm × 3 mm) was presented at the center of the screen for 1000-1500 ms, succeeded by the probe appearing at the center for 300 ms (80 mm × 80 mm), and concluding with another 600 ms blank screen. The total duration of each trial ranged from 3800 to 4800 ms (Rico-Picó et al., 2021).

2.5. EEG recording and analysis

The electroencephalogram (EEG) was recorded using the Curry 8 32-channels recording system in DC mode. Vertical electrooculogram (VEOG) electrodes were positioned at the superior and inferior orbital ridge centers on the left side, while horizontal electrooculogram (HEOG) electrodes were placed at the outer canthi of both eyes. The reference point for EEG recording was established at the midpoint between FPz and Fz. The data sampling rate was configured at 1024 Hz, with a low-pass recording bandwidth of 100 Hz. Throughout the experiment, the impedance of all electrodes was consistently maintained below 10 kΩ. EEG data processing was conducted using the EEGLAB 2019 toolbox on the MATLAB 2019b platform. During the analytical phase, the data were re-referenced to the average of all electrodes, followed by band-pass filtering within the range of 0.1–40 Hz. Bad channels were identified through meticulous visual inspection and subsequently replaced using spherical interpolation. For each participant, the interpolation of channels did not exceed 5 %. The data were segmented into two distinct phases: the cue-locked and the probe-locked, with time windows of 2400 ms and 1400 ms, respectively. The baseline for both phases was defined as the 200 ms interval preceding the stimulus. To mitigate artifacts, trials exhibiting significant drift were manually excluded. Independent component analysis (ICA) was then employed to identify and remove artifacts associated with eye movements and muscle activity. Across all participants, an average of 3 ± 3 ICA components were visually identified as artifacts and subsequently removed. Finally, segments with amplitudes exceeding ±100 μV at any electrode were discarded. To ensure the robustness of the results, event-related potentials

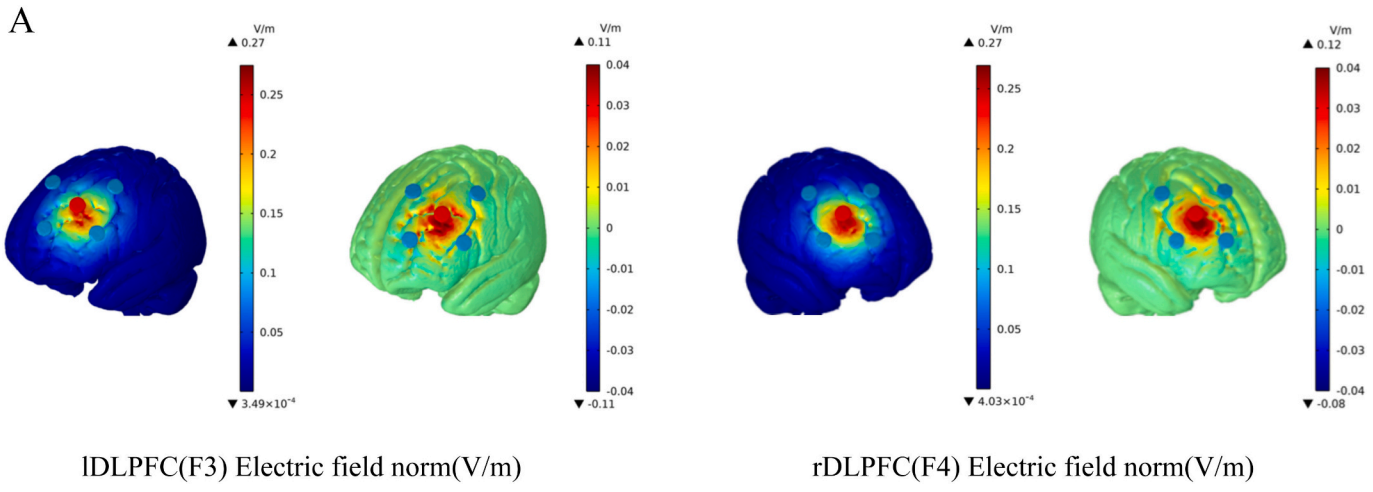

Fig. 1A. The left figure represents left DLPFC normal electric field strength. The right figure represents right DLPFC electric field strength. The normal electric field images on a plus/minus color scale to indicate inward vs. outward electric field.

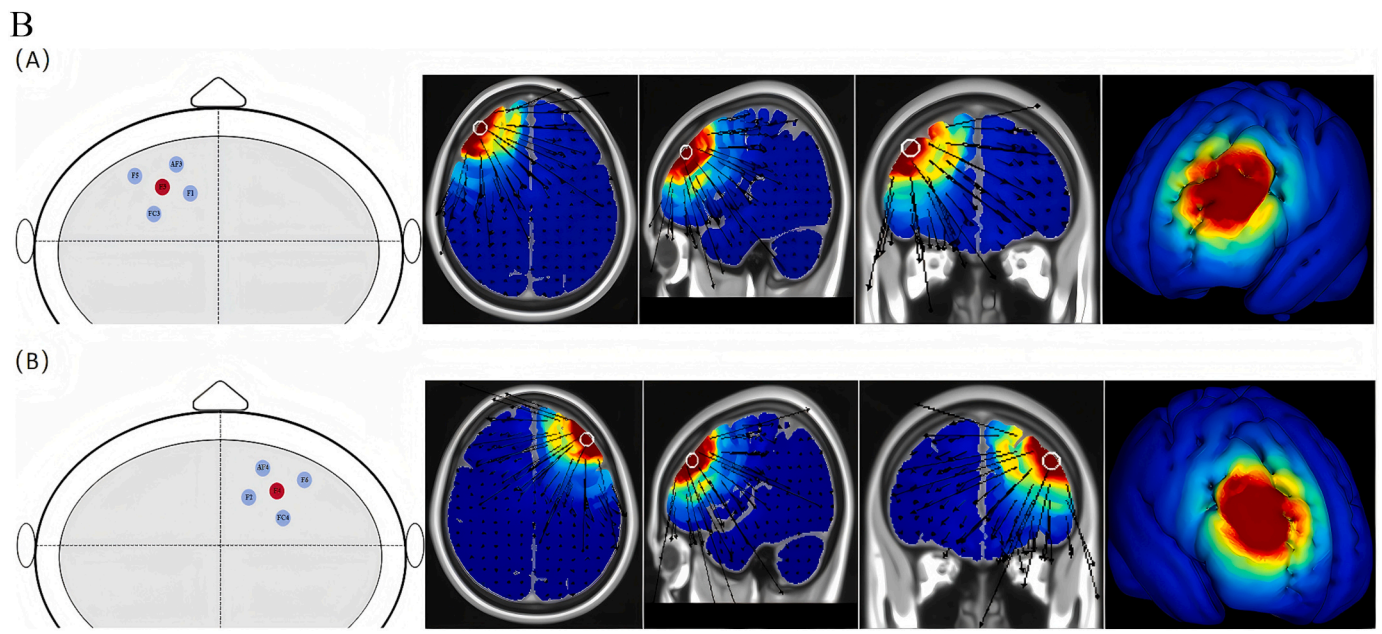

Fig. 1B. The upper figure represents stimulation electrodes setting and theoretical electronic field for left DLPFC, and electrode locations of left DLPFC(F3) corresponding return electrodes. The bottom figure represents stimulation electrodes setting and theoretical electronic field for right DLPFC, and electrode locations of right DLPFC(F4) corresponding return electrodes. The orientation of the electric field is described by the arrows in the slice plots.

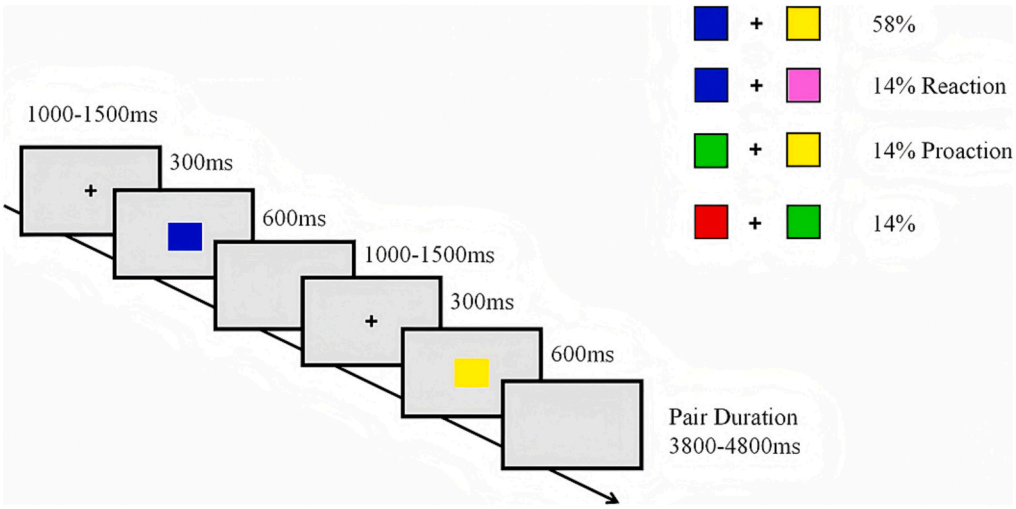

Fig. 2. Flowcharts of AX-CPT tasks and their proportions. AX pairs: the cue (A) consists of a blue square, the probe (X) is a yellow square, accounting for 58 %. AY pairs: the cue (A) consists of a blue square, the probe (Y) is a purple square, accounting for 14 %. BX pairs: the cue (B) consists of a green square, the probe (X) is a yellow square, accounting for 14 %. (For interpretation of the references to color in this figure legend, the reader is referred to the web version of this article.)

(ERPs) were computed exclusively for trials with correct task responses. The number of retained epochs did not exhibit significant differences across the various combinations (ps $>$ 0.05).

The selection of EEG analysis channels was based on previous studies. The Cz channel was designated for the analysis of the CNV, with the average amplitude in the 1500–2300 ms cue-locked time window used as the CNV index (Hämmerer et al., 2010). The FCz channel was selected for the analysis of the probe-locked N2, utilizing the 200–300 ms probe-locked time window. The Cz channel was also employed for the analysis of the post-probe P3 component, with the 450–700 ms post-probe time window designated for this purpose (Rico-Picó et al., 2021; Wessel, 2018). To enhance the signal-to-noise ratio and address the variability in peak latency across different conditions, the average amplitude within a 50 ms window centered on the N2 peak and a 125 ms window centered on the P3 peak were used for the analysis of the N2 and P3 components (Clayson et al., 2013).

2.6. Statistical analysis

All data were analyzed using SPSS 21. The final dataset comprised task accuracy rates, *d*' Context indices, and amplitudes of ERPs for both groups under three conditions: pre-test, post-sham stimulation, and post-active stimulation. A repeated-measures analysis of variance (ANOVA) was employed to analyze these data. Within-group analyses treated task pairs and stimulation conditions as within-subjects factors, while between-group analyses considered stimulation locations as between-subject factors. Main effects, interaction effects, and pairwise comparisons were examined for each condition, with all pairwise comparisons subjected to Bonferroni correction. Pearson's correlation was utilized to evaluate the relationship between ERPs and behavioral

measures. To address potential motor artifacts arising from bimanual task performance, reaction times for correct trials across conditions were computed, and no significant differences attributable to bimanual execution were found. The alpha level for statistical significance was set at $p < 0.05$.

3. Results

3.1. Behavioral results

A combined repeated-measures ANOVA was performed on the accuracy rates of both groups with a 2 (location: left, right) × 3 (condition: AX, AY, BX) × 3 (time: pre, active, sham). The results indicated a significant main effect of time, [$F(2,112) = 6.940$, $p = 0.001$, $\eta^2 = 0.110$], and a significant main effect of condition, [$F(2, 112) = 6.940$, $p < 0.001$, $\eta^2 = 0.356$]. Pairwise comparisons showed that the accuracy rate for the BX pairs in the lDLPFC group was significantly higher than that in the rDLPFC group after active stimulation, [$t(56) = 2.007$, $p = 0.050$]. Other effects were not significant, [location, $F(1, 56) = 0.881$, $p = 0.352$, $\eta^2 = 0.015$; condition × location, $F(2, 112) = 0.482$, $p = 0.619$, $\eta^2 = 0.009$; time × location $F(2, 112) = 0.278$, $p = 0.757$ $\eta^2 = 0.005$; condition × time, $F(4, 224) = 1.761$, $p = 0.138$, $\eta^2 = 0.030$; time × location× location, $F(4, 224) = 1.578$, $p = 0.181$, $\eta^2 = 0.027$].

A repeated-measures ANOVA was conducted on the accuracy rates of the lDLPFC group with a 3 (condition: AX, AY, BX) × 3 (time: pre, active, sham). The results revealed a significant main effect of time, [$F(2, 84) = 3.856$, $p = 0.025$, $\eta^2 = 0.084$]. The main effect of condition was also significant, [$F(2, 168) = 26.716$, $p < 0.001$, $\eta^2 = 0.241$]. Pairwise comparisons indicated that the accuracy rate for BX was significantly higher after active stimulation compared to pre-stimulation [$t(56) = 2.505$, $p = 0.015$] and sham stimulation [$t(56) = 2.579$, $p = 0.013$]. The interaction between time × condition was not significant, [$F(4, 168) = 0.791$, $p = 0.533$, $\eta^2 = 0.018$]. For the rDLPFC group, a repeated-measures ANOVA with the same design showed a significant main effect of condition, [$F(2, 168) = 21.650$, $p < 0.001$, $\eta^2 = 0.205$]. Other effects were not significant, [time, $F(2, 84) = 1.627$, $p = 0.203$, $\eta^2 = 0.037$; time × condition, $F(4, 168) = 1.510$, $p = 0.202$, $\eta^2 = 0.035$]. (see Fig. 3 and Table 1).

A repeated-measures ANOVA was performed on the *d*' Context indices (calculated as AX hit rate minus BX false alarm rate) using a 2 (location: left, right) × 3 (time: pre, active, sham). The analysis revealed a significant main effect of time, [$F(2, 112) = 3.329$, $p = 0.039$, $\eta^2 = 0.056$]; Other effects were not significant, [location, $F(1, 56) = 0.232$, $p = 0.632$, $\eta^2 = 0.004$; time × location, $F(2, 112) = 2.302$, $p = 0.105$, $\eta^2 = 0.039$]. Pairwise comparisons demonstrated that the *d*' in the lDLPFC group was significantly higher than that in the rDLPFC group following active stimulation[$t(56) = 2.334$, $p = 0.023$]. No significant differences were observed in the pre and sham stimulation[pre-*d*', $t(56) = -0.309$, $p = 0.758$; sham-*d*', $t(56) = -0.461$, $p = 0.647$]. Furthermore, the *d*' in the lDLPFC group was significantly elevated after active stimulation compared to both pre[$t(56) = 2.554$, $p = 0.013$] and sham stimulation[$t(56) = 2.941$, $p = 0.005$]; in the rDLPFC group no significantly differences were observed, pre compared to both sham[$t(56) = 0.254$, $p = 0.800$] and active stimulation[$t(56) = -0.070$, $p = 0.945$], sham compared to active stimulation [$t(56) = -0.349$, $p = 0.729$]. (see Fig. 4 and Table 1).

3.2. ERPs results

3.2.1. Cue-locked CNV

A combined repeated-measures ANOVA was performed on the mean CNV during the cue-locked for both groups, using a 2 (location: left, right) × 3 (condition: AX, AY, BX) × 3 (time: pre, active, sham). The results revealed a significant main effect of condition, [$F(2, 112) = 7.608$, $p = 0.001$, $\eta^2 = 0.120$]. Pairwise comparisons revealed that, following active stimulation, the CNV in the AX [$t(56) = -2.377$, $p = 0.021$] and BX [$t(56) = -3.441$, $p = 0.001$] pairs were significantly greater in the lDLPFC group compared to the rDLPFC group. No significant differences were observed in the pre and sham stimulation[pre-AX-CNV, $t(56) = -0.226$, $p = 0.822$; pre-AY-CNV, $t(56) = 0.295$, $p = 0.769$; pre-BX-CNV, $t(56) = -0.253$, $p = 0.802$; sham-AX-CNV, $t(56) = -0.396$, $p = 0.693$; sham-AY-CNV, $t(56) = -0.474$, $p = 0.637$; sham-BX-CNV, $t(56) = 0.378$, $p = 0.707$]. The time × group was significant, [$F(2, 112) = 3.196$, $p = 0.045$, $\eta^2 = 0.054$]. Simple effects analysis showed that the sum of CNV of the three conditions in the lDLPFC group was significantly greater following active stimulation compared to pre [$F(2, 55) = 3.037$, $p = 0.047$, $\eta^2 = 0.099$] and sham stimulation [$F(2, 55) = 3.037$, $p = 0.022$, $\eta^2 = 0.099$], with no significant differences observed in the rDLPFC group. The interaction between time and condition was also significant, [$F(4, 224) = 2.628$, $p = 0.035$, $\eta^2 = 0.045$]. Simple effects analysis indicated that, following active stimulation, the CNV in the BX was significantly greater than that in the pre [$F(2, 55) = 3.572$, $p = 0.038$, $\eta^2 = 0.115$] and sham stimulation [$F(2, 55) = 3.037$, $p = 0.012$, $\eta^2 = 0.115$], with no significant differences observed in the AX and AY conditions. Other effects were not significant, [time, $F(2, 112) = 0.767$, $p = 0.467$, $\eta^2 = 0.014$; location, $F(1, 56) = 1.768$, $p = 0.189$, $\eta^2 = 0.031$; condition × location, $F(2, 112) = 0.466$, $p = 0.629$, $\eta^2 = 0.008$; condition × location × time, $F(4, 224) = 1.258$, $p = 0.288$, $\eta^2 = 0.022$].

For cue-locked CNV in the lDLPFC group, ANOVA revealed a significant main effect of condition, [$F(2, 168) = 7.336$, $p = 0.001$, $\eta^2 = 0.080$]; main effect of time was not significant, [$F(2, 84) = 2.148$, $p = 0.123$, $\eta^2 = 0.049$]. The interaction between time × condition was also significant, [$F(4, 168) = 3.699$, $p = 0.007$, $\eta^2 = 0.081$]. Simple effects analysis revealed that, following active stimulation, the CNV in the BX condition was significantly greater than that in the pre [$F(2, 83) = 13.368$, $p = 0.015$, $\eta^2 = 0.111$] and sham stimulation [$F(2, 83) = 13.368$, $p = 0.003$, $\eta^2 = 0.111$]. For the rDLPFC group, ANOVA showed no significant effects, [time, $F(2, 84) = 0.387$, $p = 0.680$, $\eta^2 = 0.009$; condition, $F(2, 168) = 2.537$, $p = 0.082$, $\eta^2 = 0.029$; condition × time, $F(4, 168) = 0.378$, $p = 0.824$, $\eta^2 = 0.009$]. (see Fig. 5A and 5B; Table 2).

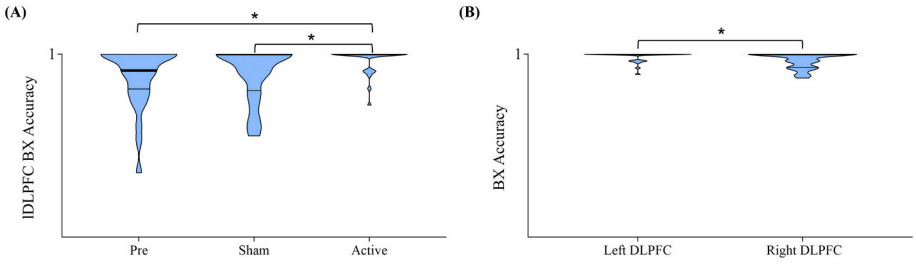

Fig. 3. Violin plots is constructed from the average accuracy of two groups of participants in three pairs after three tests. (A) The lDLPFC group demonstrated significantly highter accuracy in the BX pairs after active compared to the after pre and sham stimulation. (B) The lDLPFC group demonstrated significantly highter accuracy in the BX pairs after active compared to the rDLPFC group.*$P < 0.05$. Pre: Pre-stimulation ; Sham: Sham-stimulation ; Active: Active-stimulation; the thin lines represent quartile; the thick lines represent medians.

Table 1
The means and SD of accuracy rates and *d'* for each condition during the AX-CPT task in the two groups.

		AX	AY	BX	*d'*
Left DLPFC	Pre	0.994(0.005)	0.961 (0.036)	0.977 (0.033)	0.971 (0.034)
	Active	0.995 (0.007)	0.972 (0.035)	0.993 (0.014)	0.989 (0.016)
	Sham	0.989 (0.014)	0.963 (0.033)	0.978 (0.293)	0.968 (0.035)
Right DLPFC	Pre	0.992 (0.011)	0.955 (0.051)	0.981 (0.027)	0.974 (0.033)
	Active	0.990 (0.013)	0.972 (0.035)	0.984 (0.021)	0.974 (0.029)
	Sham	0.989 (0.010)	0.945 (0.075)	0.982 (0.205)	0.971 (0.027)

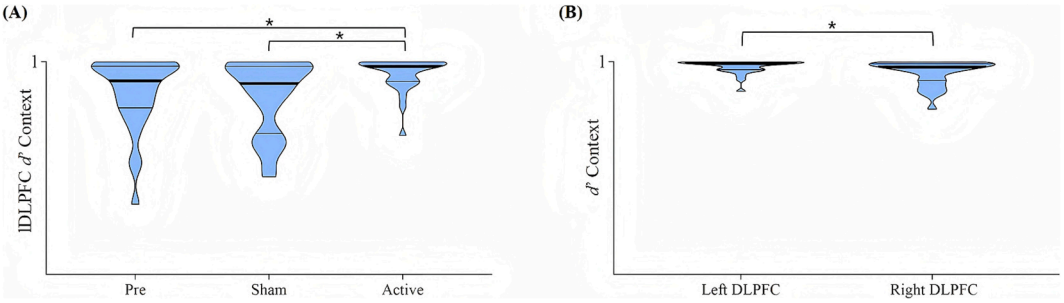

Fig. 4. Violin plots is constructed from the average *d'* of two groups of participants after three tests. (A) The lDLPFC group demonstrated significantly highter *d'* after active compared to the after pre and sham stimulation. (B) The lDLPFC group demonstrated significantly highter *d'* after active compared to the rDLPFC group. *$P <$ 0.05. Pre: Pre-stimulation ; Sham: Sham-stimulation ; Active: Active-stimulation; the thin lines represent quartile; the thick lines represent medians.

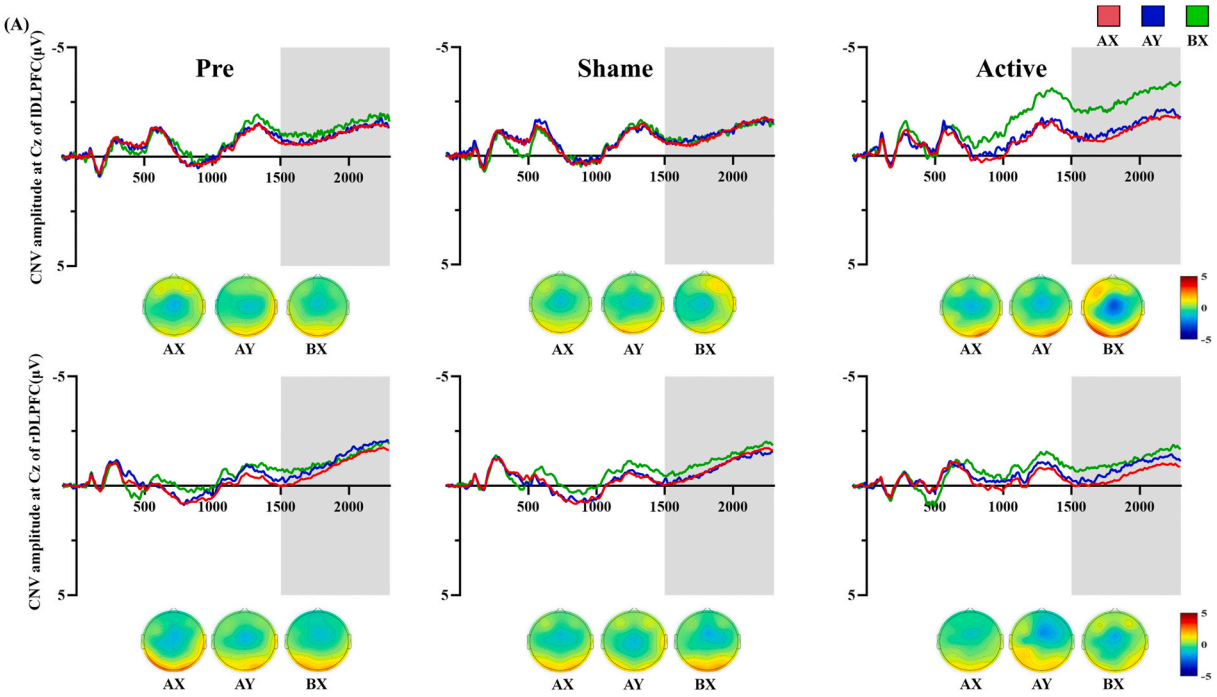

Fig. 5A. (A) Waveforms and topographical maps of CNV of lDLPFC and rDLPFC groups of participants in three conditions after three tests along Cz. Topographical maps were constructed using the mean amplitude for the CNV period (1500–2300 ms). Pre: Pre-stimulation; Sham: Sham-stimulation; Active: Active-stimulation; Gray shaded areas represent component time windows.

3.2.2. Probe-locked ERPs

A combined repeated-measures ANOVA was performed on the mean N2 during the probe-locked for both groups, using a 2 (location: left, right) × 3 (condition: AX, AY, BX) × 3 (time: pre, active, sham). The analysis revealed a significant three-way interaction among time × condition × group, [$F(4, 224) = 3.853$, $p = 0.005$, $\eta^2 = 0.064$]. Simple effects analysis indicated that, following true stimulation, the N2 in the AX was significantly smaller than that in the AY [$F(2, 55) = 7.009$, $p = 0.008$, $\eta^2 = 0.203$] and BX [$F(2, 55) = 7.009$, $p = 0.009$, $\eta^2 = 0.203$] pairs in the lDLPFC group. No significant differences were observed among the three conditions during pre and sham stimulation. All other effects were non-significant, [condition, $F(2, 112) = 1.311$, $p = 0.274$, $\eta^2 = 0.023$; time, $F(2, 112) = 0.355$, $p = 0.702$, $\eta^2 = 0.006$; location, $F(1, 56) = 0.285$, $p = 0.596$, $\eta^2 = 0.005$; condition × location, $F(2, 112) = 1.062$, $p = 0.349$, $\eta^2 = 0.019$; location × time, $F(2, 112) = 0.434$, $p = 0.649$, $\eta^2 = 0.008$; condition × time, $F(4, 224) = 1.232$, $p = 0.298$, $\eta^2 = 0.022$].

For probe-locked N2 in the lDLPFC group, ANOVA revealed no

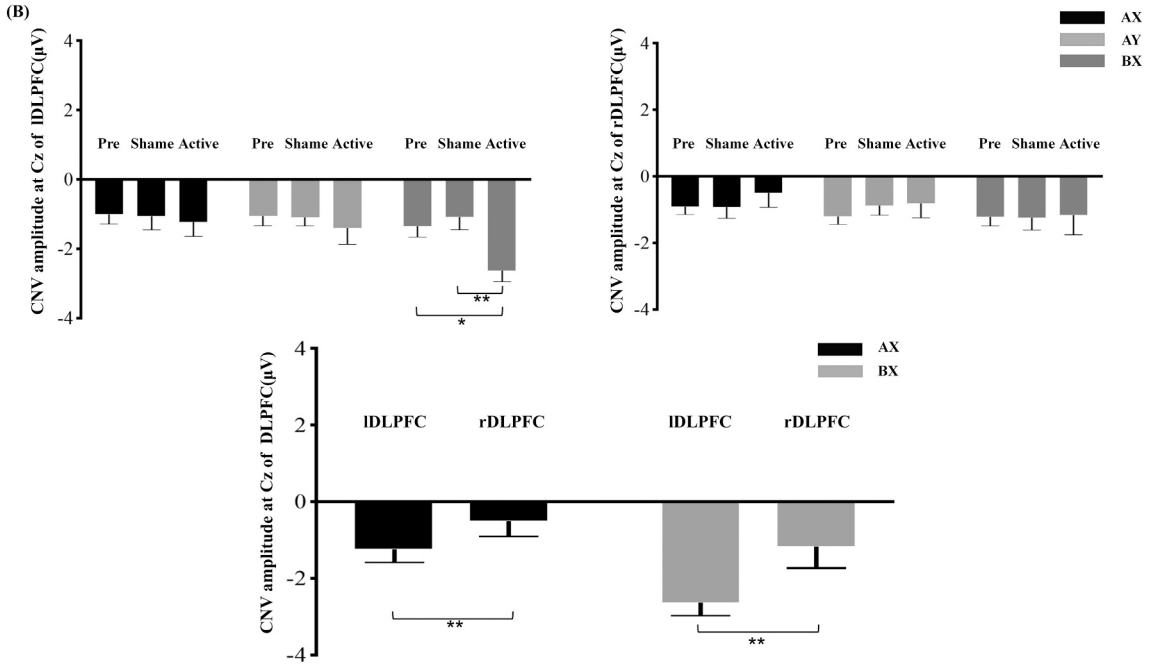

Fig. 5B. (B) Bar chart of the amplitude of CNV along the Cz channel between 1500 and 2300 ms. *$P < 0.05$; **$P < 0.01$. Pre: Pre-stimulation; Sham: Sham-stimulation; Active: Active-stimulation.

significant main effects for time, [$F(2, 84) = 0.018$, $p = 0.982$, $\eta^2 < 0.001$] and condition, [condition, $F(2, 168) = 0.920$, $p = 0.400$, $\eta^2 = 0.011$]. However, the interaction between time and condition was statistically significant, [$F(4, 168) = 2.901$, $p = 0.024$, $\eta^2 = 0.065$]. Simple effects analysis revealed that, following active stimulation, the N2 amplitude in the AX was significantly smaller than that in the AY [$F(2, 83) = 6.102$, $p = 0.006$, $\eta^2 = 0.128$] and BX [$F(2, 83) = 6.102$, $p = 0.024$, $\eta^2 = 0.128$] pairs. No significant differences were observed among the three conditions during pre and sham stimulation. For the rDLPFC group, ANOVA revealed no significant effects, [time, $F(2, 84) = 0.519$, $p = 0.597$, $\eta^2 = 0.012$; condition, $F(2, 168) = 2.940$, $p = 0.056$, $\eta^2 = 0.034$; condition × time, $F(4, 168) = 0.527$, $p = 0.716$, $\eta^2 = 0.012$]. (see Fig. 6A and 6B; Table 2).

A combined repeated-measures ANOVA was performed on the mean P3 amplitude during the cue phase for both groups, using a 2 (location: left, right) × 3 (condition: AX, AY, BX) × 3 (time: pre, active, sham) design. The analysis revealed a significant main effect of condition, [$F(2, 112) = 3.242$, $p = 0.043$, $\eta^2 = 0.055$]. Other effects were not significant, [time, $F(2, 112) = 0.417$, $p = 0.660$, $\eta^2 = 0.007$; location, $F(1, 56) = 0.150$, $p = 0.700$, $\eta^2 = 0.003$; condition × location, $F(2, 112) = 2.117$, $p = 0.125$, $\eta^2 = 0.036$; location × time, $F(2, 112) = 0.043$, $p = 0.958$, $\eta^2 = 0.001$; condition × time, $F(4, 224) = 0.773$, $p = 0.544$, $\eta^2 = 0.014$; time × condition × group, $F(4, 224) = 0.277$, $p = 0.893$, $\eta^2 = 0.005$].

For probe-locked P3 in the lDLPFC group, ANOVA revealed no significant effects, [time, $F(2, 84) = 0.244$, $p = 0.784$, $\eta^2 = 0.006$; condition, $F(2, 168) = 2.036$, $p = 0.134$, $\eta^2 = 0.024$; condition × time, $F(4, 168) = 0.524$, $p = 0.718$, $\eta^2 = 0.012$]. For the rDLPFC group, ANOVA revealed a significant main effect of condition, [$F(2, 168) = 5.897$, $p = 0.003$, $\eta^2 = 0.066$]. Other effects were not significant, [time, $F(2, 84) = 0.049$, $p = 0.952$, $\eta^2 = 0.001$; condition × time, $F(4, 168) = 0.282$, $p = 0.889$, $\eta^2 = 0.007$] (see Fig. 7A and 7B; Table 2).

3.3. Fluid intelligence score

A repeated-measures ANOVA was performed on the fluid intelligence score using a 2 (location: left, right) × 3 (time: pre, active, sham). The results revealed no significant main effects for either time [$F(2, 112) = 0.515$, $p = 0.599$, $\eta^2 = 0.009$] and group [$F(1, 56) = 0.012$, $p = 0.914$, $\eta^2 < 0.001$]. However, a statistically significant interaction effect was observed between time and group, [$F(2, 112) = 4.576$, $p = 0.012$, $\eta^2 = 0.076$]. Simple effects analysis revealed that, following active stimulation, the fluid intelligence scores in the lDLPFC group were significantly higher than those in the rDLPFC group, [$F(1, 56) = 6.325$, $p = 0.015$, $\eta^2 = 0.101$]. No significant differences were found between the two groups during the pre [$F(1, 56) = 1.506$, $p = 0.225$, $\eta^2 = 0.026$] and sham stimulation [$F(1, 56) = 0.498$, $p = 0.483$, $\eta^2 = 0.009$]. Furthermore, within the lDLPFC group, the fluid intelligence scores after active stimulation were significantly higher compared to those during pre [$t(56) = -2.466$, $p = 0.017$] and sham stimulation[$t(56) = -1.864$, $p = 0.046$]. No significant differences in fluid intelligence scores were observed in the rDLPFC group across the different stimulation conditions, pre compared to both sham[$t(56) = -0.073$, $p = 0.942$] and active stimulation[$t(56) = 1.165$, $p = 0.249$], sham compared to active stimulation [$t(56) = 1.201$, $p = 0.235$]. (see Fig. 8).

3.4. Correlation analyses

The CNV in the BX serves as a neurophysiological marker for proactive preparation of subsequent responses. Following the effective intervention of active stimulation in the lDLPFC, we conducted correlation analyses between CNV_{BX} and other indicators. The results revealed a significant positive correlation between CNV_{BX} and CNV_{AX} ($r = 0.626$, $p < 0.001$), as well as a positive correlation with the accuracy rate in the BX ($r = 0.379$, $p = 0.043$). Conversely, CNV_{BX} exhibited significant negative correlations with $N2_{AX}$ ($r = -0.536$, $p = 0.003$) and $N2_{BX}$ ($r = -0.419$, $p = 0.024$). No statistically significant correlations were observed between CNV_{BX} and the other indicators.

Following active stimulation of the lDLPFC, participants exhibited a significant improvement in fluid intelligence scores. Consequently, we calculated the correlations between fluid intelligence scores and various indicators within the lDLPFC group. The results revealed a significant negative correlation between fluid intelligence scores and the amplitude of CNV_{BX} ($r = -0.432$, $p = 0.019$). There was no significant correlation with other behaviors and ERP indicators.

Table 2
The means and SD of amplitudes for the ERP components during the AX-CPT task in the two groups.

		Cue-locked				Probe-locked							
		CNV-Cz				N2-FCz				P3-Cz			
		AX	AY	BX		AX	AY	BX		AX	AY	BX	
Left DLPFC	Pre	−0.995 (1.400)	−1.050 (1.585)	−1.352 (2.295)		−2.002 (2.176)	−1.837 (2.361)	−2.073 (1.966)		1.063 (2.225)	1.314 (2.595)	1.100 (2.215)	
	Active	−1.221 (1.147)	−1.401 (1.579)	−2.624 (1.846)		−1.408 (2.701)	−2.462 (1.913)	−1.890 (3.005)		1.244 (1.875)	1.522 (2.221)	1.768 (1.698)	
	Sham	−1.048 (1.250)	−1.099 (1.757)	−1.080 (1.628)		−2.068 (1.778)	−1.679 (2.251)	−2.313 (1.867)		1.214 (2.066)	1.518 (2.161)	1.460 (2.042)	
Right DLPFC	Pre	−0.912 (1.409)	−1.200 (2.237)	−1.213 (1.892)		−2.435 (1.315)	−2.320 (2.146)	−2.505 (1.609)		1.478 (2.771)	1.649 (2.611)	1.133 (2.069)	
	Active	−0.487 (1.205)	−0.816 (1.612)	−1.167 (1.340)		−2.269 (1.279)	−1.741 (1.470)	−2.294 (1.546)		1.514 (2.118)	1.867 (2.441)	1.416(0.945)	
	Sham	−0.916 (1.292)	−0.873 (1.864)	−1.235 (1.505)		−1.976 (1.998)	−1.868 (2.499)	−2.146 (2.134)		1.399 (2.315)	1.890 (2.410)	1.374 (2.177)	

4. Discussion

This study examined whether HD-tACS could enhance proactive control by analyzing behavioral and ERPs data from participants in the lDLPFC and rDLPFC groups during the AX-CPT paradigm under pre-stimulation, sham stimulation, and active stimulation conditions. The results demonstrated that, compared to the rDLPFC group, the lDLPFC group showed a significant improvement in proactive control following theta-frequency tACS intervention. Specifically, after active stimulation, accuracy rates in the AX and BX pairs, as well as the *d*' Context indices, were significantly higher than pre-stimulation. Furthermore, the accuracy rates and *d*' Context indices in the BX were significantly different from those of the rDLPFC group. In terms of neural indicators, the lDLPFC group exhibited a significantly increased CNV amplitude during the cue-locked under active stimulation, which is associated with proactive control and differed significantly from the rDLPFC group. During the probe-locked, the N2 in the AX was significantly reduced in the lDLPFC group. These findings indicate that HD-tACS targeting the lDLPFC significantly enhances proactive control compared to the rDLPFC group. Additionally, the efficacy of tACS intervention showed a significant transfer effect on fluid intelligence, with the lDLPFC group displaying a notable improvement in fluid intelligence scores post-active stimulation compared to both other stimulation conditions and the rDLPFC group.

The behavioral results revealed that the lDLPFC group showed a significant improvement in accuracy rates in both the AX and BX pairs following HD-tACS, with the BX accuracy rate being significantly higher than that of the rDLPFC group. Additionally, the lDLPFC group demonstrated a higher *d*' Context indices compared to the rDLPFC group. These findings are closely linked to the lDLPFC group's adoption of a more proactive cognitive strategy in the AX-CPT task after receiving 6 Hz active stimulation (Redick, 2014; Richmond et al., 2015; Wiemers and Redick, 2018). In the task, the AX sequence (58 %) occurred significantly more frequently than the BX (14 %) and AY (14 %) sequences, leading participants to develop a strong associative tendency between the cue A and the probe X. This response tendency resulted in cognitive conflict when the BX sequence appeared. For the BX, individuals leaning toward proactive control could mitigate this conflict by actively maintaining the representation of the cue B before the presentation of the probe X, which typically triggers the response tendency. As a result, proactive control is manifested in a reduced error rate in the BX (Braver, 2012). The rDLPFC group, regardless of the stimulation condition, demonstrated less efficient cue processing compared to the lDLPFC group following active stimulation. This indicates that, compared to the rDLPFC group, tACS stimulation targeting the lDLPFC enabled participants to more effectively utilize the cues provided in the task, resulting in a significant enhancement of proactive control abilities.

Studies have demonstrated that individuals' increased proactive control and preparatory focus on the BX may result in reduced accuracy rates when the AY is presented (Burgess and Braver, 2010). However, our findings reveal that the lDLPFC group exhibited an upward trend in AY accuracy following active stimulation, a pattern consistent with the performance of the rDLPFC group post-stimulation. This observation aligns with prior research. For example, Zhu et al. (2023) administered 20 min of 6 Hz high-precision tACS to the lDLPFC and demonstrated that theta-frequency stimulation significantly enhanced performance in the Stroop task, underscoring the pivotal role of the lDLPFC in reactive control. Thus, although the lDLPFC group adopted a more proactive control strategy during the task after receiving real stimulation, they also exhibited improved reactive control capabilities. These results suggest that theta-frequency tACS targeting the lDLPFC not only enhances proactive control but also facilitates reactive control, highlighting the multifaceted role of the lDLPFC in cognitive control.

The CNV is widely recognized as a neural marker of anticipatory attention (Brunia, 1999) or response preparation processes (Karayanidis

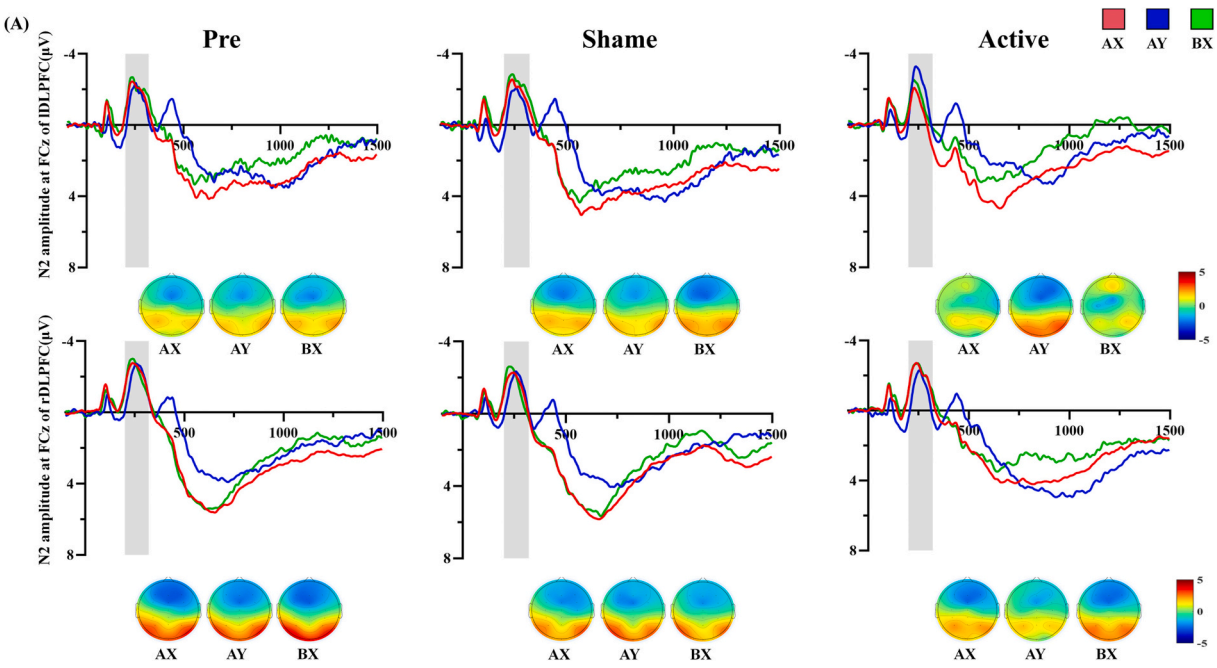

Fig. 6A. (A) Waveforms and topographical maps of N2 of lDLPFC and rDLPFC groups of participants in three conditions after three tests along FCz. Topographical maps were constructed using the mean amplitude for the N2 period (200–300 ms). Pre: Pre-stimulation; Sham: Sham-stimulation; Active: Active-stimulation; Gray shaded areas represent component time windows.

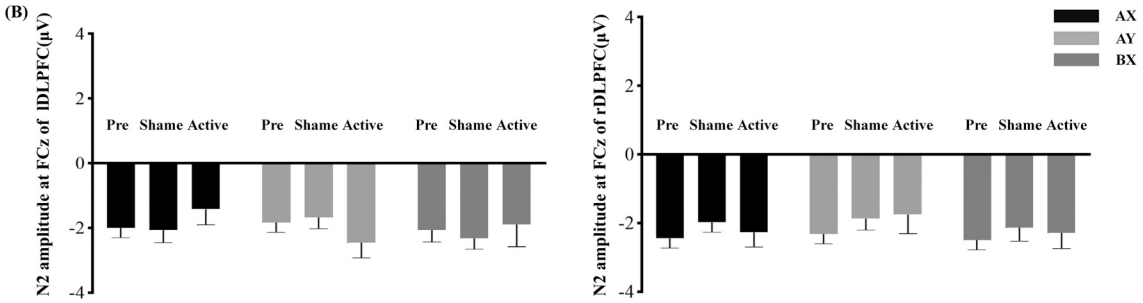

Fig. 6B. (B) Bar chart of the amplitude of N2 along the FCz channels between 200 and 300 ms. Pre: Pre-stimulation ; Sham: Sham-stimulation ; Active: Active-stimulation.

and Jamadar, 2014). In this study, we observed that the lDLPFC group exhibited a significantly larger CNV amplitude in the BX compared to the AX and AY pairs following active stimulation. Furthermore, the CNV in both the AX and BX pairs was significantly greater in the lDLPFC group than in the rDLPFC group. These results indicate that theta-frequency tACS intervention significantly enhances proactive control abilities. Previous research has demonstrated that during early childhood, proactive control can be indexed by the CNV in the AX, with larger amplitudes reflecting more robust proactive control in young children (Rico-Picó et al., 2021). As cognitive control matures, the CNV in the BX gradually supplants that in the AX as the primary neural marker of proactive control (Wang and Zhou, 2025). The findings of this study corroborate this developmental trajectory, as the CNV in the BX significantly increased post-intervention, alongside an enhancement in the AX condition CNV. This pattern may suggest that, during the initial stages of cognitive development, attentional resources are predominantly allocated to frequently encountered stimuli to manage simple tasks in daily life. As cognitive abilities mature, individuals progressively automate the processing of common stimuli and reallocate attentional resources toward understanding rules, actively maintaining them, and employing meta-cognitive strategies to address unexpected events. This adaptive shift enables individuals to more effectively select contextually appropriate responses and inhibit inappropriate ones, highlighting the dynamic evolution of proactive control across developmental stages.

The N2, a neural marker of conflict monitoring, revealed that the lDLPFC group demonstrated a significant reduction in N2 in the AX following active stimulation, both relative to their own baseline and in comparison to the rDLPFC group. The N2 is widely regarded as a cognitive component of anterior cingulate cortex (ACC) activation. Within the DMC, the ACC plays a pivotal role in both proactive and reactive control strategies (Braver et al., 2007). Specifically, when individuals employ a proactive control strategy, the ACC facilitates top-down attentional processes and enhances preparatory mechanisms for subsequent responses. Additionally, the ACC's role in conflict monitoring supports the detection and resolution of conflicts during reactive control (Jimura et al., 2010; Paxton et al., 2008). As previously noted, the AX can also serve as an indicator of proactive control abilities to some extent. Integrating the observed trends in N2 amplitude changes in the BX and AY pairs across different stimulation conditions in the lDLPFC group, along with their high correlation, this study provides partial support for the DMC. Specifically, when individuals exhibit robust proactive control abilities, the ACC is activated during the cue-locked, prompting the allocation of greater attentional resources to actively maintain the internal representation of task cues. Due to this

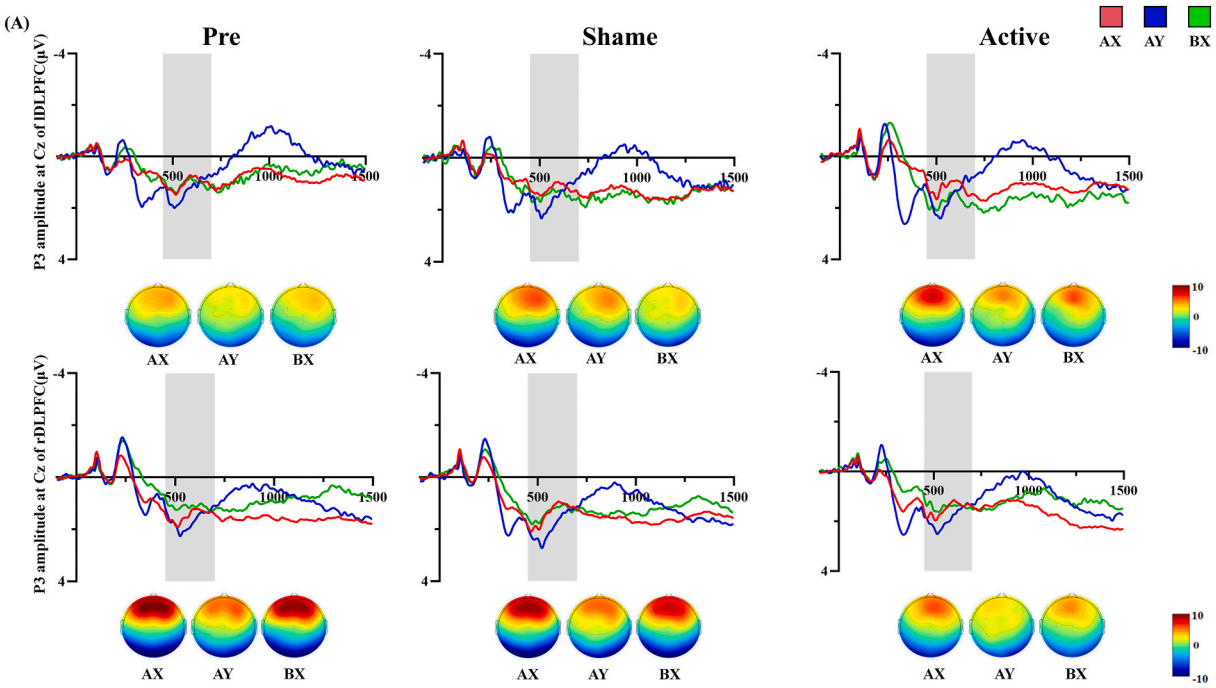

Fig. 7A. (A) Waveforms and topographical maps of P3 of rDLPFC and rDLPFC groups of participants in three conditions after three tests along Cz. Topographical maps were constructed using the mean amplitude for the N2 period (450–700 ms). Pre: Pre-stimulation; Sham: Sham-stimulation; Active: Active-stimulation; Gray shaded areas represent component time windows.

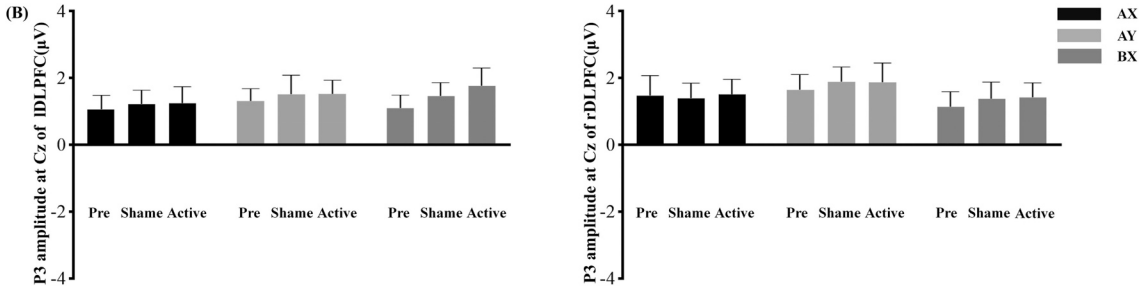

Fig. 7B. (B) Bar chart of the amplitude of P3 along the Cz channels between 450 and 700 ms. Pre: Pre-stimulation; Sham: Sham-stimulation; Active: Active-stimulation.

proactive cue maintenance, individuals require less conflict monitoring during the probe-locked, resulting in diminished ACC activation and a smaller N2 at this stage.

The P3 component is widely recognized as a neural marker of inhibitory costs during cognitive control processes. In this study, we observed larger P3 in the AY, consistent with previous findings (Liu et al., 2011). This phenomenon may be attributed to the presence of the A cue, which primes participants for subsequent stimuli, suggesting that unexpected conflicts necessitate stronger reactive inhibition, thereby increasing inhibitory costs. However, no significant changes in P3 were detected in the BX following the active intervention, potentially indicating that the intervention did not fully exploit the latent plasticity of proactive control. Researche shows that applying 20 min of 2 mA transcranial direct current stimulation (tDCS) to the DLPFC in patients with schizophrenia significantly altered error rate patterns, increased gamma power, and enhanced proactive control abilities (Boudewyn et al., 2020). These findings suggest that proactive control is not only associated with theta frequency but also intricately linked to gamma frequency. The multiple buffers model proposes that short-term information is represented by the ordered activity of cell assemblies, and the maintenance of multiple items in working memory is facilitated by gamma subcycles nested within theta oscillations. A central tenet of this model is that distinct gamma subcycles, corresponding to different theta phases, enable the maintenance and segregation of information through oscillatory activity (Lisman and Jensen, 2013). When theta oscillation peaks are coupled with the energy of high-frequency gamma oscillations (80–100 Hz), spatial working memory performance is significantly enhanced, and overall neocortical connectivity is strengthened. Moreover, cross-frequency tACS stimulation has been shown to yield superior outcomes compared to single-frequency stimulation (Alekseichuk et al., 2016). Consequently, the stimulation protocol employed in this study may have inherent limitations. Future research exploring cross-frequency tACS interventions could elucidate the neural signatures of proactive control and further investigate its underlying plasticity.

The results showed that stimulation of the lDLPFC with HD-tACS increased individual proactive control without any change in individual proactive control with tACS stimulation of the rDLPFC. Previous studies have shown that neuromodulation interventions in the lDLPFC increase self-control behaviors, such as enhanced delayed gratification, reduced gambling-seeking, and reduced risk-taking tendencies (Gilmore et al., 2018; Guo et al., 2018; Nejati et al., 2018). Our results further suggest the causal implication of lDLPFC in proactive control, extending

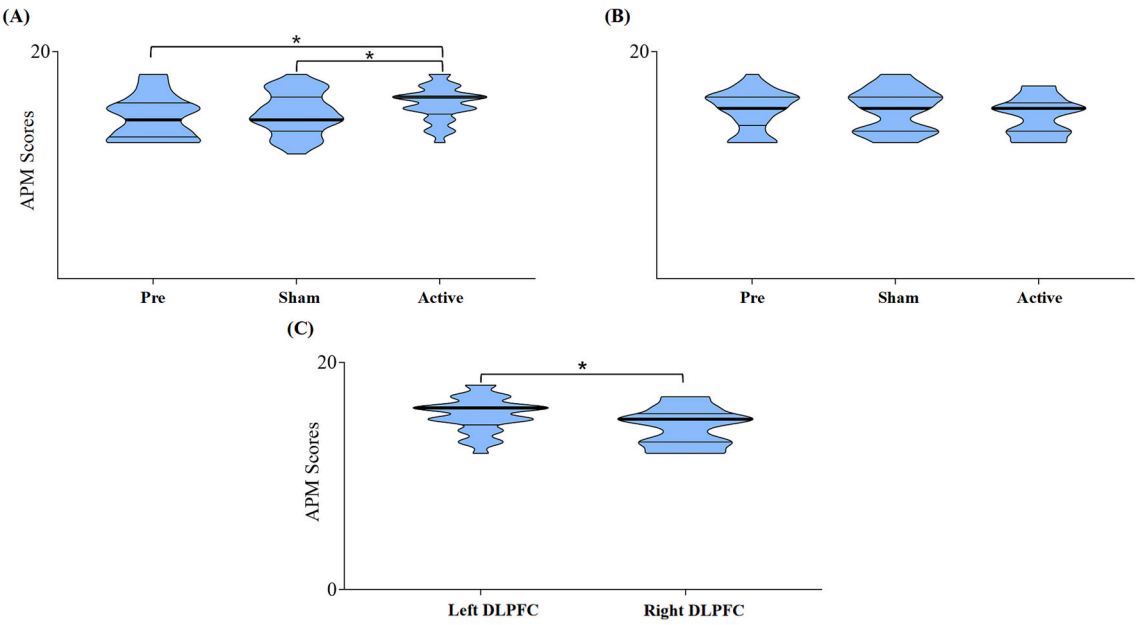

Fig. 8. Violin plots is constructed from the average fluid intelligence score of two groups of participants after three tests. (A) The lDLPFC group demonstrated significantly highter scores after active compared to the after pre and sham stimulation; (B) The rDLPFC group showed no significant difference in scores after active compared to the after pre and sham stimulation; (C) The lDLPFC group demonstrated significantly highter scores after active compared to the rDLPFC group. *$P < 0.05$. Pre: Pre-stimulation; Sham: Sham-stimulation; Active: Active-stimulation; the thin lines represent quartile; the thick lines represent medians.

previous perspectives that self-control behavior is related to lDLPFC morphology or connectivity (Chen et al., 2020; Liu and Feng, 2017; Xu et al., 2021). For the non-significant effect of rDLPFC, this study cannot completely rule out its role in proactive control ability, and we provide possible insights into the specific role rDLPFC may play in proactive control ability in the future. Whether there are systemic differences in the function of the DLPFC on different sides remains controversial. For example, several studies have proposed that the rDLPFC plays a key role in negative emotion regulation (Feeser et al., 2014; Heller et al., 2013), which may have the potential to active regulation of aversive task execution. Addressing the neural correlates of self-control behavior, some studies have found that a relationship between behavioral control and spontaneous activity or structural changes in the rDLPFC (Wang et al., 2022; Zhang et al., 2016) is possibly mediated by emotion regulation or cognitive control. Moreover, studies have shown that inhibition of rDLPFC activation can impair individual's proactive control ability (Gomez-Ariza et al., 2017). To this end, more exploratory studies are still needed before reaching a laterality-specific conclusion about roles of DLPFC in proactive control as well as its underlying pathway.

The different roles played by lDLPFC and rDLPFC in proactive control ability further influence the transfer effect of fluid intelligence. Following theta-frequency tACS stimulation, participants in the lDLPFC group demonstrated not only a marked enhancement in proactive control but also a positive transfer effect to individual fluid intelligence. Analysis of correlations between fluid intelligence scores and other metrics within the lDLPFC group revealed a significant positive correlation with the CNV in the BX post-active stimulation. This phenomenon may be attributed to the substantial overlap in neural networks underlying both cognitive faculties (Rueda, 2018). Dosenbach et al. in their examination of brain functional connectivity, introduced a dual-network model of cognitive control (Dosenbach et al., 2007; Dosenbach et al., 2008). The FPN, which is integral to response inhibition, also occupies a pivotal role in the parieto-frontal integration theory (P-FIT) of intelligence. This network underpins the co-evolution of cognitive control and fluid intelligence, with the DLPFC emerging as a critical informational nexus within this network (Fjell et al., 2015; Vendetti and Bunge, 2014). Consequently, effective intervention targeting proactive control has been observed to positively influence individual fluid intelligence scores. Nonetheless, certain studies posit that this transfer may be confined to elementary fluid intelligence assessments, suggesting that the parietal lobe constitutes the essential node for augmenting individual fluid intelligence (Pahor and Jaušovec, 2014). The intricate relationship between individual proactive control capabilities and fluid intelligence warrants further comprehensive investigation at the whole-brain level.

Our results are consistent with the hypothesis, demonstrating that theta-frequency HD-tACS stimulation targeting the lDLPFC can effectively enhance proactive control in individuals, with the intervention effects positively transferring to fluid intelligence, thereby improving fluid intelligence scores. The AX-CPT is a widely utilized task for assessing cognitive control, motor preparation, anticipation, and sustained attention, among other processes. Within this paradigm, the preparatory period between the presentation of the cue and the stimulus can be delineated into three distinct stages: sensory input, cue evaluation, and motor preparation. Following the presentation of cue B, neural oscillations during these stages are characterized by a significant reduction in alpha oscillations within the prefrontal cortex. This reduction may reflect the anticipatory attentional mechanism for action processing after individuals receive task cues (Bickel et al., 2012). Furthermore, studies have demonstrated that theta-frequency tACS stimulation targeting the lDLPFC significantly diminishes alpha oscillations (Pahor and Jaušovec, 2014). Concurrently, neural theta oscillations facilitate the rapid allocation of attentional and related cognitive resources (Jaušovec and Jaušovec, 2014). The confluence of these two factors may constitute a pivotal mechanism underlying the efficacy of this intervention. Research underscores that the adoption and efficiency of proactive control strategies during task execution are intricately intertwined with the development of working memory. Working memory, defined as the capacity to maintain and manipulate information over brief intervals, is posited to rely on at least two functionally independent subsystems: the executive system and the representational system. The former orchestrates the allocation of cognitive resources to task-relevant information and prioritizes the processing and retrieval of pertinent representations, while the latter sustains the specific content of task-relevant information (Baddeley, 2003). The interplay between these systems, which are thought to depend on distinct neural

substrates, particularly the frontal and parietal cortices, is essential for working memory. Cross-regional information exchange is hypothesized to be mediated by theta-band neural oscillations, with prefrontal theta activity modulating parietal engagement associated with the maintenance of working memory content. Theta oscillations may serve as a critical mechanism coordinating the interaction between the frontal executive system and the parietal representational system (Ratcliffe et al., 2022).

In summary, this study extends prior research by investigating the plasticity of proactive control in individuals. The findings demonstrate that tACS effectively enhances proactive control abilities. However, the study is subject to certain limitations. Notably, the absence of control groups receiving other single-frequency stimulations precludes definitive conclusions regarding the specificity of theta-frequency stimulation in improving proactive control. Furthermore, participants were exclusively composed of university students, and the lack of age-diverse control groups leaves unresolved whether tACS-induced plasticity generalizes across different age ranges. The division of participants into two groups also introduces potential confounding of the results. Research demonstrates that cross-frequency stimulation yields superior effects compared to single-frequency stimulation, prompting the need for further exploration of proactive control plasticity through cross-frequency approaches. While event-related potential (ERP) technology provides high temporal resolution, offering robust neural indices for examining the proactive control process, its limited spatial resolution constrains a more comprehensive understanding of this relationship. Future research should address these limitations to refine our understanding of the mechanisms underlying proactive control plasticity. In addition, the DLPFC plays a key role in emotion regulation, especially in the suppression of negative emotional responses. It helps individuals to reduce emotional overreactions by modulating the activity of other brain areas related to emotional responses, such as the amygdala and anterior cingulate cortex, thus contributing to the effective management of emotions (Aydın, 2022, 2023). Therefore, the ability of neuromodulation to intervene in individuals' emotion regulation is also currently a focus of future attention.

5. Conclusion

This study provides evidence that theta-frequency tACS applied to the lDLPFC significantly enhances proactive control in individuals, while also revealing a dynamic relationship between proactive control and fluid intelligence. These results revealed the critical role of the lDLPFC as a neural substrate for proactive control and highlight the potential of neural oscillation modulation as a intervention for enhancing higher-order cognitive functions.

CRediT authorship contribution statement

Lei Wang: Writing – review & editing, Writing – original draft, Validation, Methodology, Formal analysis, Data curation, Conceptualization. **YuHong Ou:** Writing – original draft, Formal analysis, Data curation. **Renlai Zhou:** Writing – review & editing, Writing – original draft, Supervision, Project administration, Funding acquisition, Conceptualization.

Declaration of competing interest

None.

Acknowledgments

This work was supported by Space Medical Experiment Project of China Manned Space Program (HYZHXMR01006). We would like to express our gratitude for the support of the project.

Data availability

Data will be made available on request.

References

Alekseichuk, I., Turi, Z., Amador de Lara, G., Antal, A., Paulus, W., 2016. Spatial working memory in humans depends on Theta and high gamma synchronization in the prefrontal cortex. Curr. Biol. 26 (12), 1513–1521.
Amin, Z., Epperson, C.N., Constable, R.T., Canli, T., 2006. Effects of estrogen variation on neural correlates of emotional response inhibition. NeuroImage 32 (1), 457–464.
Antal, A., Boros, K., Poreisz, C., Chaieb, L., Terney, D., Paulus, W., 2008. Comparatively weak after-effects of transcranial alternating current stimulation (tACS) on cortical excitability in humans. Brain Stimul. 1 (2), 97–105.
Aydın, S., 2022. Cross-validated Adaboost classification of emotion regulation strategies identified by spectral coherence in resting-state. Neuroinformatics 20 (3), 627–639.
Aydın, S., 2023. Investigation of global brain dynamics depending on emotion regulation strategies indicated by graph theoretical brain network measures at system level. Cogn. Neurodyn. 17 (2), 331–344.
Baddeley, A., 2003. Working memory: looking back and looking forward. Nat. Rev. Neurosci. 4 (10), 829–839.
Bickel, S., Dias, E.C., Epstein, M.L., Javitt, D.C., 2012. Expectancy-related modulations of neural oscillations in continuous performance tasks. Neuroimage 62 (3), 1867–1876.
Boudewyn, M.A., Scangos, K., Ranganath, C., Carter, C.S., 2020. Using prefrontal transcranial direct current stimulation (tdcs) to enhance proactive cognitive control in schizophrenia. Neuropsychopharmacology 45 (11), 1–9.
Braver, T.S., 2012. The variable nature of cognitive control: a dual mechanisms framework. Trends Cogn. Sci. 16 (2), 106–113.
Braver, T.S., Gray, J.R., Burgess, G.C., 2007. Explaining the many varieties of working memory variation: Dual mechanisms of cognitive control. In: Conway, A.R.A., Jarrold, C., Kane, M.J., Miyake, A., Towse, J.N. (Eds.), Variation in Working Memory. Oxford University Press, Oxford, pp. 76–106.
Braver, T.S., Paxton, J.L., Locke, H.S., Barch, D.M., 2009. Flexible neural mechanisms of cognitive control within human prefrontal cortex. Proc. Natl. Acad. Sci. USA 106 (18), 7351–7356.
Bruin, K.J., Wijers, A.A., 2002. Inhibition, response mode, and stimulus probability: a comparative event-related potential study. Clin. Neurophysiol. 113 (7), 1172–1182.
Brunia, C.H.M., 1999. Neural aspects of anticipatory behavior. Acta Psychol. 101 (2–3), 213–242.
Burgess, G.C., Braver, T.S., 2010. Neural mechanisms of interference control in working memory: effects of interference expectancy and fluid intelligence. PLoS One 5 (9), e12861.
Burgess, G.C., Gray, J.R., Conway, A.R.A., Braver, T.S., 2011. Neural mechanisms of interference control underlie the relationship between fluid intelligence and working memory span. J. Exp. Psychol. Gen. 140 (4), 674–692.
Casey, B.J., Giedd, J.N., Thomas, K.M., 2000. Structural and functional brain development and its relation to cognitive development. Biol. Psychol. 54 (1–3), 241–257.
Cavanagh, J.F., Frank, M.J., 2014. Frontal theta as a mechanism for cognitive control. Trends Cogn. Sci. 18 (8), 414–421.
Chen, Z., Liu, P., Zhang, C., Feng, T., 2020. Brain morphological dynamics of procrastination: the crucial role of the self-control, emotional, and episodic prospection network. Cereb. Cortex 30 (5), 2834–2853.
Church, J.A., Bunge, S.A., Petersen, S.E., Schlaggar, B.L., 2017. Preparatory engagement of cognitive control networks increases late in childhood. Cerebral Cortex(3), 2139–2153.
Clayson, P.E., Baldwin, S.A., Larson, M.J., 2013. How does noise affect amplitude and latency measurement of event-related potentials (ERPs)? A methodological critique and simulation study. Psychophysiology 50 (2), 174–186.
Cocchi, L., Zalesky, A., Fornito, A., Mattingley, J.B., 2013. Dynamic cooperation and competition between brain systems during cognitive control. Trends Cogn. Sci. 17 (10), 493–501.
Cohen, J.D., Barch, D.M., Carter, C., Servan-schreiber, D., 1999. Context-processing deficits in schizophrenia: converging evidence from three theoretically motivated cognitive tasks. J. Abnorm. Psychol. 108 (1), 120–133.
Court, J.H., Raven, J., 1995. Manual for Raven's progressive matrices and vocabulary scales. Section 7: Research and references: Summaries of normative, reliability, and validity studies and references to all sections. Psychologists Press, Oxford, England: Oxford.
Diamond, A., 2013. Executive functions. Annu. Rev. Psychol. 64, 135–168.
Dosenbach, N.U.F., Fair, D.A., Miezin, F.M., Cohen, A.L., Wenger, K.K., Dosenbach, R.A. T., Petersen, S.E., 2007. Distinct brain networks for adaptive and stable task control in humans. Proc. Natl. Acad. Sci. 104 (26), 11073–11078.
Dosenbach, N.U.F., Fair, D.A., Cohen, A.L., Schlaggar, B.L., Petersen, S.E., 2008. A dual-networks architecture of top-down control. Trends Cogn. Sci. 12 (3), 99–105.
Edwards, B.G., Barch, D.M., Braver, T.S., 2010. Improving prefrontal cortex function in schizophrenia through focused training of cognitive control. Front. Hum. Neurosci. 4, 32.
Eisma, J., Rawls, E., Long, S., Mach, R., Lamm, C., 2021. Frontal midline theta differentiates separate cognitive control strategies while still generalizing the need for cognitive control. Sci. Rep. 11 (1), 14641.
Feeser, M., Prehn, K., Kazzer, P., Mungee, A., Bajbouj, M., 2014. Transcranial direct current stimulation enhances cognitive control during emotion regulation. Brain Stimul. 7 (1), 105–112.

Fjell, A.M., Westlye, L.T., Amlien, I., Tamnes, C.K., Grydeland, H., Engvig, A., Walhovd, K.B., 2015. High-expanding cortical regions in human development and evolution are related to higher intellectual abilities. Cereb. Cortex 25 (1), 26–34.
Force, R.B., Riddle, J., Jarskog, L.F., Frhlich, F., 2021. A case study of the feasibility of weekly tacs for the treatment of auditory hallucinations in schizophrenia. Brain Stimul. 14 (2), 361–363.
Gilmore, C.S., Dickmann, P.J., Nelson, B.G., Lamberty, G.J., Lim, K.O., 2018. Transcranial direct current stimulation (tDCS) paired with a decision-making task reduces risk-taking in a clinically impulsive sample. Brain Stimul. 11 (2), 302–309.
Goense, J.B., Logothetis, N.K., 2008. Neurophysiology of the BOLD fMRI signal in awake monkeys. Curr. Biol. : CB 18 (9), 631–640. https://doi.org/10.1016/j.cub.2008.03.054.
Gomez-Ariza, C.J., Martín, M.C., Morales, J., 2017. Tempering proactive cognitive control by means of tdcs of the lateral prefrontal cortex. Brain Stimul. 10 (2), 360.
Guo, H., Zhang, Z., Da, S., Sheng, X., Zhang, X., 2018. High-definition transcranial direct current stimulation (HD-tDCS) of left dorsolateral prefrontal cortex affects performance in balloon analogue risk task (BART). Brain Behav. 8 (2), e00884.
Hämmerer, D., Li, S.C., Müller, V., Lindenberger, U., 2010. An electrophysiological study of response conflict processing across the lifespan: assessing the roles of conflict monitoring, cue utilization, response anticipation, and response suppression. Neuropsychologia 48 (11), 3305–3316.
Heller, A.S., Johnstone, T., Peterson, M.J., Kolden, G.G., Kalin, N.H., Davidson, R.J., 2013. Increased prefrontal cortex activity during negative emotion regulation as a predictor of depression symptom severity trajectory over 6 months. JAMA Psychiatry 70 (11), 1181–1189.
Jacobs, J., Hwang, G., Curran, T., Kahana, M.J., 2006. EEG oscillations and recognition memory: theta correlates of memory retrieval and decision making. NeuroImage 32 (2), 978–987.
Jaušovec, N., Jaušovec, K., 2012. Working memory training: improving intelligence–changing brain activity. Brain Cogn. 79 (2), 96–106.
Jaušovec, N., Jaušovec, K., 2014. Increasing working memory capacity with theta transcranial alternating current stimulation (tacs). Biol. Psychol. 96, 42–47.
Jimura, K., Locke, H.S., Braver, T.S., 2010. Prefrontal cortex mediation of cognitive enhancement in rewarding motivational contexts. Proc. Natl. Acad. Sci. USA 107 (19), 8871–8876.
Karayanidis, F., Jamadar, S.D., 2014. Event-related potentials reveal multiple components of proactive and reactive control in task switching. In: Grange, J.A., Houghton, G. (Eds.), Task Switching and Cognitive Control. Oxford University Press, New York, pp. 200–236.
Klimesch, W., Hanslmayr, S., Sauseng, P., Gruber, W., Brozinsky, C.J., Kroll, N.E., Yonelinas, A.P., Doppelmayr, M., 2006. Oscillatory EEG correlates of episodic trace decay. Cereb. Cortex 16 (2), 280–290.
Koch, S.P., Werner, P., Steinbrink, J., Fries, P., Obrig, H., 2009. Stimulus-induced and state-dependent sustained gamma activity is tightly coupled to the hemodynamic response in humans. The Journal of neuroscience : the official journal of the Society for Neuroscience 29 (44), 13962–13970. https://doi.org/10.1523/JNEUROSCI.1402-09.2009.
Li, Y., Liu, F., Zhang, Q., Liu, X., Wei, P., 2018. The effect of mindfulness training on proactive and reactive cognitive control. Front. Psychol. 9, 1002.
Lisman, J.E., Jensen, O., 2013. The theta-gamma neural code. Neuron 77 (6), 1002–1016.
Liu, P., Feng, T., 2017. The overlapping brain region accounting for the relationship between procrastination and impulsivity: a voxel-based morphometry study. Neuroscience 360, 9–17.
Liu, T., Xiao, T., Shi, J., Zhao, D., 2011. Response preparation and cognitive control of highly intelligent children: a go-Nogo event-related potential study. Neuroscience 180, 122–128.
Lo, S.L., 2018. A meta-analytic review of the event-related potentials (ern and n2) in childhood and adolescence: providing a developmental perspective on the conflict monitoring theory. Dev. Rev. 48, 82–112.
Macar, F., Vidal, F., Casini, L., 1999. The supplementary motor area in motor and sensory timing: evidence from slow brain potential changes. Exp. Brain Res. 125, 271–280.
MacDonald 3rd, A.W., Cohen, J.D., Stenger, V.A., Carter, C.S., 2000. Dissociating the role of the dorsolateral prefrontal and anterior cingulate cortex in cognitive control. Science 288 (5472), 1835–1838.
Miller, E.K., Cohen, J.D., 2001. An integrative theory of prefrontal cortex function. Annu. Rev. Neurosci. 24 (1), 167–202.
Mizuhara, H., Yamaguchi, Y., 2007. Human cortical circuits for central executive function emerge by theta phase synchronization. NeuroImage 36 (1), 232–244.
Nejati, V., Salehinejad, M.A., Nitsche, M.A., 2018. Interaction of the left dorsolateral prefrontal cortex (l-DLPFC) and right orbitofrontal cortex (OFC) in hot and cold executive functions: evidence from transcranial direct current stimulation (tDCS). Neuroscience 369, 109–123.
Nieuwenhuis, S., Yeung, N., Wildenberg, W., Ridderinkhof, K.R., 2003. Electrophysiological correlates of anterior cingulate function in a go/no-go task: effects of response conflict and trial type frequency. Cogn. Affect. Behav. Neurosci. 3 (1), 17–26.
Pahor, A., Jaušovec, N., 2014. The effects of theta transcranial alternating current stimulation (tACS) on fluid intelligence. International journal of psychophysiology: official journal of the International Organization of Psychophysiology 93 (3), 322–331.
Paxton, J.L., Barch, D.M., Storandt, M., Braver, T.S., 2006. Effects of environmental support, and strategy training on older adults' use of context. Psychol. Aging 21 (3), 499–509.
Paxton, J.L., Barch, D.M., Racine, C.A., Braver, T.S., 2008. Cognitive control, goal maintenance, and prefrontal function in healthy aging. Cereb. Cortex 18 (5), 1010–1028.
Pfefferbaum, A., Ford, J.M., Weller, B.J., Kopell, B.S., 1985. ERPs to response production and inhibition. Electroencephalogr. Clin. Neurophysiol. 60 (5), 423–434.
Pires, L., Leitão, J., Guerrini, C., Simões, M.R., 2014. Event-related brain potentials in the study of inhibition: cognitive control, source localization and age-related modulations. Neuropsychol. Rev. 24 (4), 461–490.
Ratcliffe, O., Shapiro, K., Staresina, B.P., 2022. Fronto-medial theta coordinates posterior maintenance of working memory content. Curr. Biol. 32 (10), 2121–2129.e3.
Raven, J.C., 1990. Advanced progressive matrices: Sets I, II. Oxford: Oxford Univ Press.
Redick, T.S., 2014. Cognitive control in context: working memory capacity and proactive control. Acta Psychol. 145 (1), 1–9.
Richmond, L.L., Redick, T.S., Braver, T.S., 2015. Remembering to prepare: the benefits (and costs) of high working memory capacity. J. Exp. Psychol. Learn. Mem. Cogn. 41 (6), 1764–1777.
Rico-Picó, J., Hoyo, A., Guerra, S., Conejero, A., Rueda, M.R., 2021. Behavioral and brain dynamics of executive control in relation to children's fluid intelligence. Intelligence 84, 1–11.
Rizzuto, D.S., Madsen, J.R., Bromfield, E.B., Schulze-Bonhage, A., Kahana, M.J., 2006. Human neocortical oscillations exhibit theta phase differences between encoding and retrieval. NeuroImage 31 (3), 1352–1358.
Rueda, M.R., 2018. Attention in the heart of intelligence. Trends in Neuroscience and Education 13, 26–33.
Sakai, K., Passingham, R.E., 2006. Prefrontal set activity predicts rule-specific neural processing during subsequent cognitive performance. J. Neurosci. 26 (4), 1211–1218.
Sauseng, P., Griesmayr, B., Freunberger, R., Klimesch, W., 2010. Control mechanisms in working memory: a possible function of EEG theta oscillations. Neurosci. Biobehav. Rev. 34 (7), 1015–1022.
Shen, A., Zhao, W., Han, B., Zhang, Q., Zhang, Z., Chen, X., Li, J., 2018. The contribution of the contingent negative variation (CNV) to goal maintenance. Schizophr. Res. 195, 372–377.
Smith, J.L., Johnstone, S.J., Barry, R.J., 2006. Effects of pre-stimulus processing on subsequent events in a warned go/NoGo paradigm: response preparation, execution and inhibition. Int. J. Psychophysiol. 61 (2), 121–133.
Sternberg, R.J., Ferrari, M., Clinkenbeard, P., Grigorenko, E.L., 1996. Identification, instruction, and assessment of gifted children: a construct validation of a triarchic model. Gift. Child Q. 40, 129–137.
Tavakoli, A.V., Yun, K., 2017. Transcranial alternating current stimulation (tACS) mechanisms and protocols. Front. Cell. Neurosci. 11, 214.
Thair, H., Holloway, A.L., Newport, R., Smith, A.D., 2017. Transcranial direct current stimulation (tDCS): a beginner's guide for design and implementation. Front. Neurosci. 11, 641.
Van Veen, V., Carter, C.S., 2002. The tinning of action-monitoring processes in the anterior cingulate cortex. J. Cogn. Neurosci. 14 (4), 593–602.
Vendetti, M.S., Bunge, S.A., 2014. Evolutionary and developmental changes in the lateral frontoparietal network: a little goes a long way for higher-level cognition. Neuron 84 (5), 906–917.
Walter, W.G., Cooper, R., Aldridge, V.J., et al., 1964. Contingent negative variation: an electric sign of sensorimotor association and expectancy in the human brain. Nature 203, 380–384.
Wang, J., Zhang, R., Feng, T., 2022. Neural basis underlying the association between expressive suppression and procrastination: the mediation role of the dorsolateral prefrontal cortex. Brain Cogn. 157, 105832.
Wang, L., Zhou, R., 2025. Deficits of proactive control in individuals with test anxiety: evidence from ERPs. Biol. Psychol. 194, 108985.
Wessel, J.R., 2018. Prepotent motor activity and inhibitory control demands in different variants of the go/no-go paradigm. Psychophysiology 55, 3.
Wiemers, E.A., Redick, T.S., 2018. Working memory capacity and intra-individual ariability of proactive control. Acta Psychol. 182, 21–31.
Wischnewski, M., Alekseichuk, I., Opitz, A., 2022. Neurocognitive, physiological, and biophysical effects of transcranial alternating current stimulation. Trends Cogn. Sci. 27, 189–205.
Xu, T., Sirois, F.M., Zhang, L., Yu, Z., Feng, T., 2021. Neural basis responsible for self-control association with procrastination: right MFC and bilateral OFC functional connectivity with left dlPFC. J. Res. Pers. 91, 104064.
Zhang, H., Watrous, A.J., Patel, A., Jacobs, J., 2018. Theta and alpha oscillations are traveling waves in the human neocortex. Neuron 98 (6), 1269–1281 e1264.
Zhang, W., Wang, X., Feng, T., 2016. Identifying the neural substrates of procrastination: a resting-state fMRI study. Sci. Rep. 6 (1), 33203.
Zhang, Y., Li, Q., Wang, Z., Liu, X., Zheng, Y., 2017. Temporal dynamics of reward anticipation in the human brain. Biol. Psychol. 128, 89–97.
Zhu, Y., Wu, D., Sun, K., Chen, X., Wang, Y., He, Y., Xiao, W., 2023. Alpha and theta oscillations are causally linked to interference inhibition: evidence from high-definition transcranial alternating current stimulation. Brain Sci. 13 (7), 1026.
Zink, N., Lenartowicz, A., Markett, S., 2021. A new era for executive function research: on the transition from centralized to distributed executive functioning. Neurosci. Biobehav. Rev. 124, 235–244.